

SUBMITTED VERSION

FAST TRACK PAPER

Fault and magmatic interaction within Iceland's western rift over the last 9 kyr

J. M. Bull^{1*}, T. A. Minshull¹, N. C. Mitchell², K. Thors³, J. K. Dix¹, A.I. Best¹

¹Southampton Oceanography Centre, Southampton SO14 3ZH, UK

²Earth Sciences, Cardiff University, PO Box 914, Cardiff CF10 3YE, UK

³Jardfraedistofa, Borgartun 18, 105 Reykjavik, Iceland

- ^{*}To whom correspondence should be addressed. Email: bull@soton.ac.uk

SUMMARY

We present high-resolution “Chirp” sub-bottom profiler data from Thingvallavatn, a lake in Iceland’s western rift zone. These data are combined with stratigraphic constraints from sediment cores to show that movement on normal faults since 9 ka are temporally correlated with magmatic events, indicating that movements were controlled by episodic dike intrusion. Sediment depo-centres and the focus of subsidence migrated westwards over 3 – 4 kyrs towards the locus of subsequent brittle failure. We interpret this subsidence as related to dike intrusion a few

kilometers along strike, originating from the Hengill volcanic system, which occurred prior to major diking, faulting and subsidence within the lake at 1.9 ka.

Key words: Tectonics, Faulting, Volcanic Activity, Iceland.

INTRODUCTION

Extension of the Earth's lithosphere at rift zones commonly results in both faulting and magmatism. Extension rates are stable over thousands to millions of years, but faulting and magmatism are episodic. The relationship between these processes may be unravelled by detailed studies of fault-controlled sedimentation. Here we determine the evolution of the rift zone in SW Iceland (representing the plate boundary between the North American and Eurasian plates), within the northern part of lake Thingvallavatn (Fig. 1), since 9 ka.

In rift zones, dikes intruded laterally at shallow levels can trigger normal faulting and subsidence (Saemundsson 1992; Brandsdottir and Einarsson 1979; Sigurdsson 1980). Observations of dike intrusion causing fault slip are becoming increasingly common. Analysis of dike intrusion at Kilauea volcano, Hawaii demonstrated by field observations and measurements from InSAR, reveal coeval slip on a normal fault system (Cervelli et al., 2002). Elastic models, which specify dikes and faults as planar cracks, have successfully modelled surface displacements associated with individual dike intrusion events from northern Iceland (Rubin 1992; Rubin and Pollard 1988), and Hawaii (Pollard *et al.* 1983). These models show how inflation of a magma-filled crack at depth causes crustal dilation above the dike, leading to rifting and subsidence. The dilation at the surface produces the commonly observed dike-parallel bands of fissuring and faulting.

The models are also able to reproduce the magnitudes of surface displacement. More sophisticated models incorporating individual faults that can accommodate shear displacements are able to reproduce the actual surface movements associated with individual intrusion events. In this paper we draw on the results of this modelling to explain observations of faulting, subsidence and changes in the locus of sedimentation within Thingvallavatn.

GEOLOGICAL BACKGROUND

Thingvallavatn has existed since the end of the last Ice Age. The lake is dominantly spring-fed and drains via a narrow opening in the south-eastern corner of the lake. The rift zone is dominated by faults and fissures trending N 27-29° E. The faults and fissures have opened transtensionally to the relative plate motion between Eurasia and North America, which is at 19 mm yr⁻¹ in the direction N105°E according to the NUVEL-1A model (DeMets *et al.* 1994; Alex *et al.* 1999). The most recent GPS Geodetic campaign (Alex *et al.* 1999), for the period 1992-1995 found that although the orientation of the velocity vectors fitted well with the NUVEL-1A model prediction, the magnitude was too small. Fissure swarms surrounding the lake (Gudmundsson 1987; Saemundsson 1992) are related to Hengill and associated volcanic systems. The Thingvellir fissure swarm (most prominent at the Almannagja, Fig. 1) is linked to the Hengill volcanic system by the continuity of faults and fissures (Saemundsson 1992). Tryggvason (1982) summarised measurements of present day extension and derived an average extension of 3 mm yr⁻¹ across the rift and subsidence of 1 mm yr⁻¹ of the rift centre.

In Thingvallavatn tephra layers, intercalated with diatomaceous sediments, overlie a lava which represents “acoustic” basement. The age of these sediments is well known from radiometric dating of the tephras. The rates of extension and subsidence are similar to the sedimentation rate, so the sediments record fault movements with high fidelity. Therefore the lake is an ideal natural laboratory for studying rift development.

The northern and eastern parts of Thingvallavatn are floored (acoustic basement) by the Thingvallahraun lava flow (Saemundsson 1992; Thors 1992; Fig. 1) which flowed from the north and has been dated to 9.14 ± 0.26 ka (Kjartansson 1964). Elsewhere in the lake acoustic basement is represented by the Sandey ash cone, hyaloclastite materials, and by the 1.89 ± 0.06 kyr Nesjahraun lava which flowed from the flanks of Hengill synchronously with the eruption of Sandey (Saemundsson 1992; Fig. 1). The simultaneous eruption of the Nesjahraun lava and formation of the Sandey scoria cone demonstrates sub-surface feeding of magma (diking) from the Hengill volcanic system north-eastwards to Sandey.

There is very little surface inflow of sediments into the lake, and therefore the sedimentation is dominantly pelagic with minor wind-blown dust and volcanic particles (Haflidason *et al.* 1992). A 6 m piston core (Fig. 1) taken from Thingvallavatn recovered diatomaceous sand interdigitated with at least 38 tephra layers. One of these tephras has been identified as Katla K-E at a depth of 5.2 m within the core (Hardardottir 1999). Katla K-E is typically 2 – 5 cm in thickness around Thingvallavatn and has been dated at 2.84 – 2.86 ka (Robertsdottir 1992), suggesting a sedimentation rate of 1.8 mm yr^{-1} at the core site. Sedimentation rates of 0.4 - 2.4 mm yr^{-1} , since 1.1 ka, were inferred from eight short (maximum length 0.8 m) gravity cores with the higher rates systematically

occurring in deeper water (Haflidason *et al.* 1992). Fine parallel diatomite laminations within the cores indicate weak to negligible bottom currents, although the absence of sediment in water depths shallower than 30 m suggests the presence of stronger currents around the edges of the lake. The maximum total sediment thickness is about 25 m (Fig 2) and occurs 1 km to the east of the present deepest part of the lake. Since sedimentation is currently most rapid in the deepest area, this observation suggests that the lakebed relief has changed over time. Acoustic impedances were computed from seismic velocity and density measurements on the 6 m sediment core. The impedance series was differentiated, convolved with the Chirp source signal and processed in the same way as the profiles, see later, to produce a synthetic seismogram. This seismogram suggests that acoustic impedance changes at the depth of the K-E event should give rise to a characteristic strong reflector, which is observed in the Chirp records. This reflector (representing an age of c. 3 ka) and acoustic basement (representing the 9.1 ka lava) within the northern part of the lake constrain the stratigraphic record of the lake floor.

DATA AND PRELIMINARY INTERPRETATION

The lake (Fig. 1) was initially surveyed by Thors (1992) with a boomer system and analogue sidescan sonar. That survey was unable to record details of the sedimentary history but revealed some tantalising geology. The new survey described here was carried out with a Chirp sub-bottom profiler (Quinn *et al.* 1998) and a 100 kHz sidescan sonar. The Chirp data (2-8 kHz swept source) produce a single-fold seismic section with a shot interval, for this dataset, of 0.6 – 0.8 m. The Chirp data processing included

correlation, instantaneous amplitude conversion, deconvolution, dynamic signal-to-noise filter, and coherency filtering (Quinn *et al.* 1998).

The lake (Fig 1.) has a pronounced deep (greater than 100 m) west of Sandey. The majority of the lake has water depths of 40–80 m. The faults within the lake have an orientation $N27.6^{\circ} \pm 4.3^{\circ}E$. Prominent scarps representing the lava front of the Thingvallahraun lava are clearly seen in sidescan sonar images. The east-west orientation of this front west of Sandey, where the front is cut by later rift-parallel faults, indicates that the rift had little topographic relief there at the time of the emplacement of the lava. Furthermore, the presence of the lava further south in the eastern lake provides additional evidence that the deepest part of the lake was further east at 9 ka than at present. To the south, the 1.9 ka Nesjahraun lava had a very different mode of flow to the Thingvallahraun lava (Thors 1992): it was rapidly emplaced as a slide and has no flow front. Liquefaction structures possibly linked with the impact of this lava with pre-existing sediments are seen in the profiler records.

TECTONIC AND VOLCANIC INTERPRETATION OF STRATIGRAPHY

Here we concentrate on an area north of Sandey where the stratigraphy best records the evolution of the lake, and where the 9.1 ka lava provides a uniform-age acoustic basement (Fig. 2). We discuss our results in terms of the numbered faults of Fig. 2. Our new data locate major easterly dipping faults at the western margin of the lake basin (F1-4 in Fig. 2), and a segmented eastern margin fault (F10a,b) which dips westwards. There is a major change in structural style across the line X–Y (Fig. 2) where fault F3 bifurcates

(forming F1), fault F10 is offset into separate segments F10a and F10b, and there is a change in the general dip of acoustic basement from gently dipping to the east (in the north, Fig. 3a and 3b), to dipping to the west (Fig. 3c). The major rift-bounding fault F3, displaces the Thingvallavatn lava by up to 55 m in the region south of the line X-Y. The displacement on F3 decreases sharply north of this line to 20 – 25 m. Overall there is an abrupt depression of the rift floor by 25 – 30 m south of where the change in planform of faulting occurs. Fault segments F10a and F10b represent the major eastern rift-bounding fault and have a maximum displacement of 40 m.

We illustrate changes in structural style with three representative Chirp profiles (Fig. 3). In the northernmost profile (Fig. 3a), pelagic sediment can be clearly seen with the greatest thickness within 1 km of the eastern margin fault (F10). Fault F3 represents the western margin fault, but sediment does not appear to thicken towards it on this profile. Between the two bounding faults, the lava surface dips towards to the east.

In profile B (Fig. 3b), relief on the western part of the graben is partitioned between two faults (F1 and F3), whereas the relief to the east is still accommodated by fault F10. Intervals between acoustic reflectors change abruptly across the faults within the rift centre. The reflector orientations change from dipping parallel to basement at depth, to near horizontal at the surface, a tendency that we attribute to deformation of the older reflectors. These characteristics show that the stratigraphy records the evolution of the fault system.

South of the line X–Y, the graben is distinctly asymmetrical with relief on the eastern bounding fault F10 much less than on the western bounding faults (Fig 3c.). Within the

rift floor the lava surface dips to the west. There is less relief on F10 and more on F3 than in profiles further north. The greatest thickness of sediments occurs mid-way between F3 and F10, but away from the deepest water depths. This observation contrasts with the evidence from gravity cores for increasing present-day sedimentation rate with increasing water depth (Haflidason *et al.* 1992). We infer that fault F3 has moved recently and that there has been little time for sediments to accumulate. Using the sedimentation rate results discussed earlier, the relatively thin sediment thickness in the hanging-wall of fault F3 would have accumulated since 1.5 – 2.0 ka.

Four horizons (Fig. 3c, inset) could be traced around the survey area. The deepest (yellow) represents acoustic basement (9.1 ka lava). The brown horizon overlies an acoustically transparent zone, and the basement-brown interval thins towards the foot-wall of faults. Assuming constant sedimentation rates, the age of the brown horizon is probably 5–6 ka. The purple horizon is strongly reflective, and by correlation from the 6m core (Fig. 1) corresponds to Katla event K-E at c. 3 ka. The orange horizon is the lower of a characteristic acoustic doublet which sub-parallel the sea-bed and post-dates liquefaction phenomena due to the emplacement of the 1.9 ka lava in the southern part of the lake. Assuming constant sedimentation rates, the age of the orange horizon is c. 1.5 ka.

From 9.1 ka to 5-6 ka (Fig. 4; isopach I), sedimentation was concentrated in the hanging-walls of faults F6 to F9. We interpret the thickest isopachs in the centre as indicating that this was the deepest part of the lake with sedimentation rate controlled by water depth as near to the present (Haflidason *et al.* 1992). Between 5-6 ka and 3 ka (Fig. 4; isopach II) only parts of fault F9 were active, and deposition was concentrated further west in the

hanging-walls of faults F5 – F7. During 3 – 1.5 ka (Fig. 4; isopach III) sediment was deposited more uniformly, and fault F7 was less active. Since 1.5 ka (Fig. 4; isopach IV) depositional centres have appeared along the large western boundary faults (F4 in particular), although there is still some concentrated deposition elsewhere (on F6, for example). It is difficult to say from the isopachs alone when F10 developed its present relief, but the migration of the locus of sedimentation to the west over time suggests to us that it was probably most active during the earlier period I when the depo-centre was nearby. If F10's development was linked to magmatic activity, it may be associated with the Eldborgir fissure swarm lying to the east of Figure 1, as described by Saemundsson (1992).

Isopach maps show no evidence for lateral propagation of faults within the centre of the rift as the very rapid appearance of the fault planform over 2 – 3 kyr following the emplacement of the Thingvallahruan lava requires unrealistically high propagation rates. We infer that the faults were active before the 9.1 ka lava was emplaced and that they simply broke through the thin lava crust, preserving their pre-9.1 ka lengths. Details in the sediment isopachs (Fig. 4) probably represent episodic movements on individual segments of the fault system. Because further lengthening of these faults is not resolved by our data, we infer that lengthening must be less than 25 mm yr^{-1} .

DISCUSSION

In the above section the following key observations have been made. First, fault F3 which is currently the major western margin fault, moved recently at c. 1.5 – 2.0 ka, facilitating rapid subsidence of 25 – 30 m. Second, the sediment isopach maps demonstrate a

systematic movement of the locus of sedimentation westwards towards fault F3 from 6 ka to 1.5 ka. Third, the planform of faulting changes dramatically across line X-Y (Fig. 2), and it is south of this line that fault F3 accumulated displacement rapidly 1.5 – 2 ka. Here we discuss these observations in the light of recent modelling of dike/rift systems.

Clearly, we have no direct observations of dike emplacement during this ancient event. Recent studies, however, provide a clear set of criterion for dike-detection which we apply to Iceland. Simple elastic models (without fault discontinuities) reveal that above an inflating vertical dike, the crust dilates symmetrically above the dike, while the ground surface immediately above the dike is not displaced. The result at the surface can be a broad zone of faulting and fissuring above the zone of dike intrusion, or two parallel bands of extension. Rubin (1992) and Rubin and Pollard (1988) incorporated dikes and faults as planar cracks to successfully reproduce surface displacements, and investigated different combinations of dike intrusion and fault slip that produced acceptable fits to changes in surface elevation across rift zones in Iceland. By modelling the change in horizontal stress and slip tendency on faults after dike intrusion, they showed that faults far from the dike are within a zone of dike-induced compression and are effectively locked during the dike event, whereas faults that would intersect the dike close to its top will slip until they intersect the dike at depth.

However, the amount of slip produced by dike-induced faulting is too small to explain the observed data. The remainder of the subsidence required to fit the observed data occurs by slip on the faults *laterally* ahead of the propagating dikes, where induced compression has not locked the faults at depth. The position of pre-existing faults relative to the propagating dike will control whether slip will occur.

Of particular relevance to Thingvallavatn is the modelled fit to data from Kelduhverfi (Krafla, northern Iceland). The observed subsidence (0.5 – 0.7 m) was matched by modelling two faults bounding the graben and a vertical dike in the centre, with the faults intersecting the dike at depth (Rubin 1992). Models predict significant faulting and resulting subsidence *in front* of the *laterally* propagating dikes, together with asymmetry in the graben floor (his Fig. 5).

The sudden large displacement accumulation on fault F3 has a timing consistent with the eruption of the Nesjahraun lava and the formation of the Sandey scoria cone, and we argue that the three events are linked. We further infer that the change in rift morphology between figures 3b and 3c, and the change in the planform of faulting across the line X-Y (Fig. 2), are due mostly to movement of fault F3 (but also the eastern bounding fault F10). We argue that all of these observations can be explained by the propagation of one or more dikes at depth at 1.9 ka between the Hengill volcanic system and Sandey. Fault F3 moved in front of this propagating dike (in agreement with the modelling of Rubin, 1992). Additionally, the change in geometry between profiles shown in Fig. 3b and Fig. 3c, and the overall geometry of Fig. 3c, with the asymmetrical rift floor (the Thingvallavatn lava), is similar to the simulations of the 1978 Iceland event. Assuming that the subsidence is as large as the dike width (Rubin 1992), then a 25–30 m dike, or more likely a series of thinner dikes totalling 25-30 m thickness, would have been necessary to produce the observed subsidence in Fig 3c.

The systematic movement of the sediment depo-centre westwards since at least 5 – 6 ka can also be attributed to dike injection. The migration towards the line along which the major Nesjahraun-Sandey eruptive event occurred was caused by distal subsidence ahead

of intruding dikes that originated from Hengill. The major diking event occurred at 1.9 ka, and the excess pressure associated with this diking led to the Sandey eruptive event.

CONCLUSIONS

From our high-resolution study of syn-rift stratigraphy in Iceland's western rift we conclude that:

1. Faulting and subsidence (laterally) ahead of diking associated with the emplacement of the Sandey scoria cone at 1.9 ka have been the dominant controls on the morphological evolution of the rift centred around Thingvallavatn.
2. The rift has grown mainly by rapid faulting and subsidence associated with dike intrusion, accentuated by the effect of on-going plate boundary extension.
3. Sediment depo-centres migrated systematically towards the locus of subsequent brittle failure over the preceding 3-4 kyr.

ACKNOWLEDGEMENTS

This project was supported by the Royal Society and the equipment used was funded by the Natural Environment Research Council under research grant GR3/9533. Royal Society University Research Fellowships supported TAM and NCM. We are grateful to Bryndis Brandsdottir for originally suggesting the lake as an interesting target, and to Robert Bacon and Guy Hall for early help in data processing.

REFERENCES

- Alex, N., Einarsson P., M. Heinert, W. Niemeyer, B. Ritter, F. Sigmundsson, St. Willgalis, 1999. GPS-Messkampagne 1995 zur Bestimmung von Deformationen der Erdkruste in Sudwestisland, *Zeitschrift fur Vermessungswesen.*, **124**, 347-361.
- Brandsdottir, B., and Einarsson, P., 1979. Seismic activity associated with the September 1977 deflation of Krafla volcano in north-eastern Iceland, *J. Volcanol. Geotherm. Res.*, **6**, 197-212.
- Cervelli, P., Segall, P., Amelung, F., Garbeil, H., Meertens, C., Owen, S., Miklius, A., and Lisowski, M., 2002. The September 12, 1999 Upper East Rift Zone dike intrusion at Kilauea Volcano, Hawaii. *J. Geophys. Res.*, **106**, DOI 10.1029/2001JB000602.
- DeMets, C., Gordon, R.G., Argus, D.F., and Stein, S., 1994. Effect of recent revisions to the geomagnetic reversal time scale on estimates of current plate motions, *Geophys. Res. Lett.*, **21**, 425-478.
- Gudmundsson, A., 1987. Tectonics of the Thingvellir fissure swarm, SW Iceland, *J. Struct. Geol.*, **9**, 61-69.
- Hardardottir, J., 1999. Late Weichselian and Holocene environmental history of south and west Iceland as interpreted from studies of lake and terrestrial sediments. PhD Thesis, University of Colorado, Boulder.
- Haflidason, H., Larsen, G., Olafsson, G., 1992. The recent sedimentation history of Thingvallavatn, Iceland, *Oikos* **64**, 80-95.

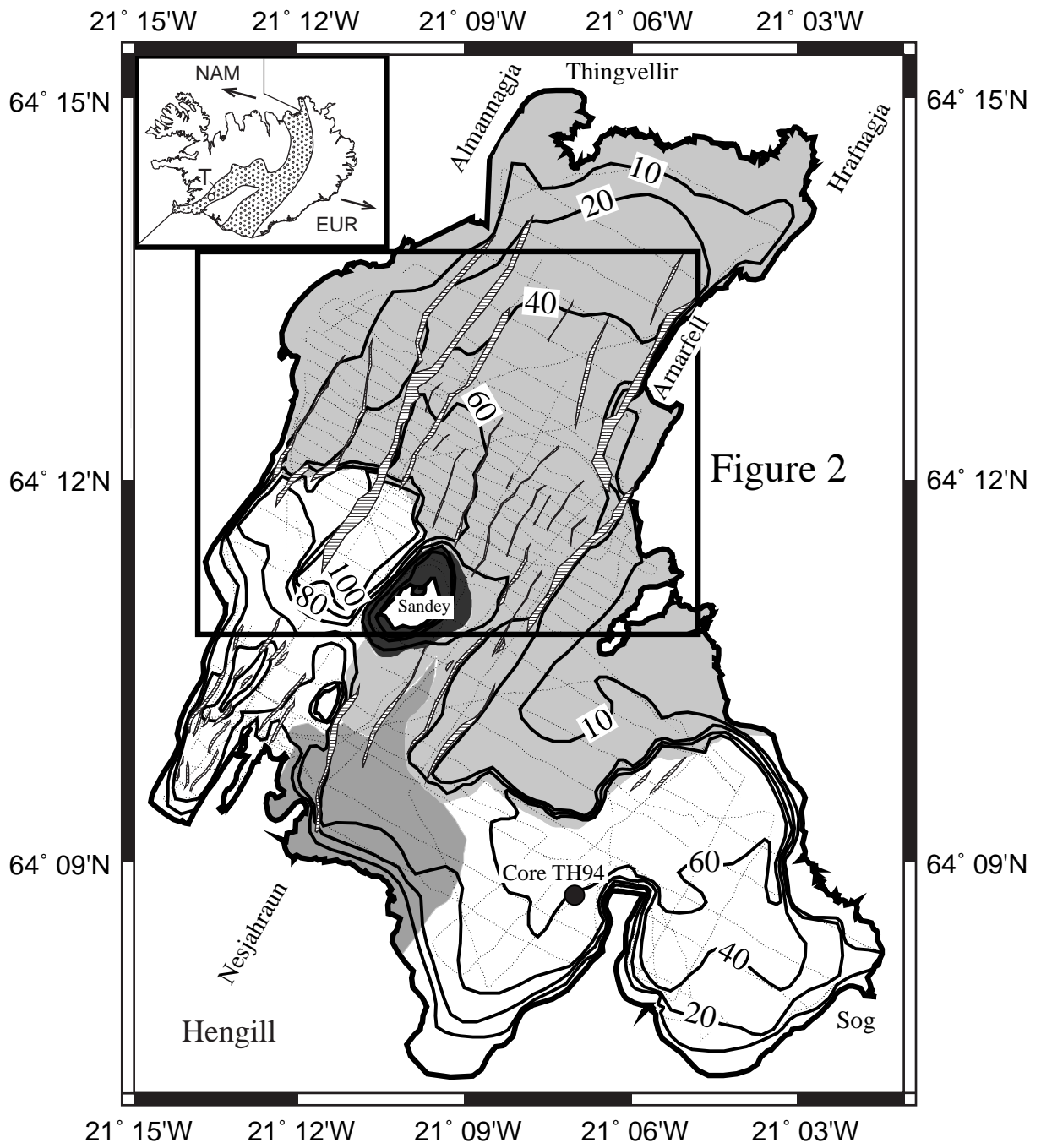
- Kjartansson, G., 1964. The retreat of the last glacial ice sheet and some volcanoes in the Kjolur area, *Naturufraedingurinn*, **34**, 101 – 113.
- Pollard, D.D., Delaney, P.T., Duffield, W.A., Endo, E.T., and Okamura, A.T., 1983. Surface deformation in volcanic rift zones, *Tectonophys.*, **94**, 541-584.
- Quinn, R., Bull, J.M. and Dix, J.K., 1998. Optimal processing of marine high-resolution seismic reflection (Chirp) data. *Mar. Geophys. Res.*, **20**, 13-20.
- Robertsdottir, B.G., 1992, Forsoguleg gjoskulog fra Kotlu, adur nefnd “Katla 5000”. Geological Society of Iceland – spring meeting, Abstracts, Reykjavik, 8-9.
- Rubin, A.M., 1992 Dike-induced faulting and graben subsidence in volcanic rift zones, *J. Geophys. Res.*, **97**, 1839-1858.
- Rubin, A.M., and Pollard, D.D., 1988. Dike-induced faulting in rift zones of Iceland and Afar, *Geology*, **16**, 413-417.
- Saemundsson, K., 1992. Geology of the Thingvallavatn area, *Oikos*, **64**, 40-68.
- Sigurdsson, O., 1980. Surface deformation of the Krafla fissure swarm in two rifting events, *J. Geophys.*, **47**, 154-159.
- Thors, K., 1992. Bedrocks, sediments, and faults in Thingvallavatn. *Oikos*, v. 64, p. 69-79.
- Tryggvason, E., 1982. Recent ground deformation in continental and oceanic rift zones. In: G. Palmason (eds), *Continental and Oceanic Rifts*. AGU Geodynamic Series **8**, 17-29.

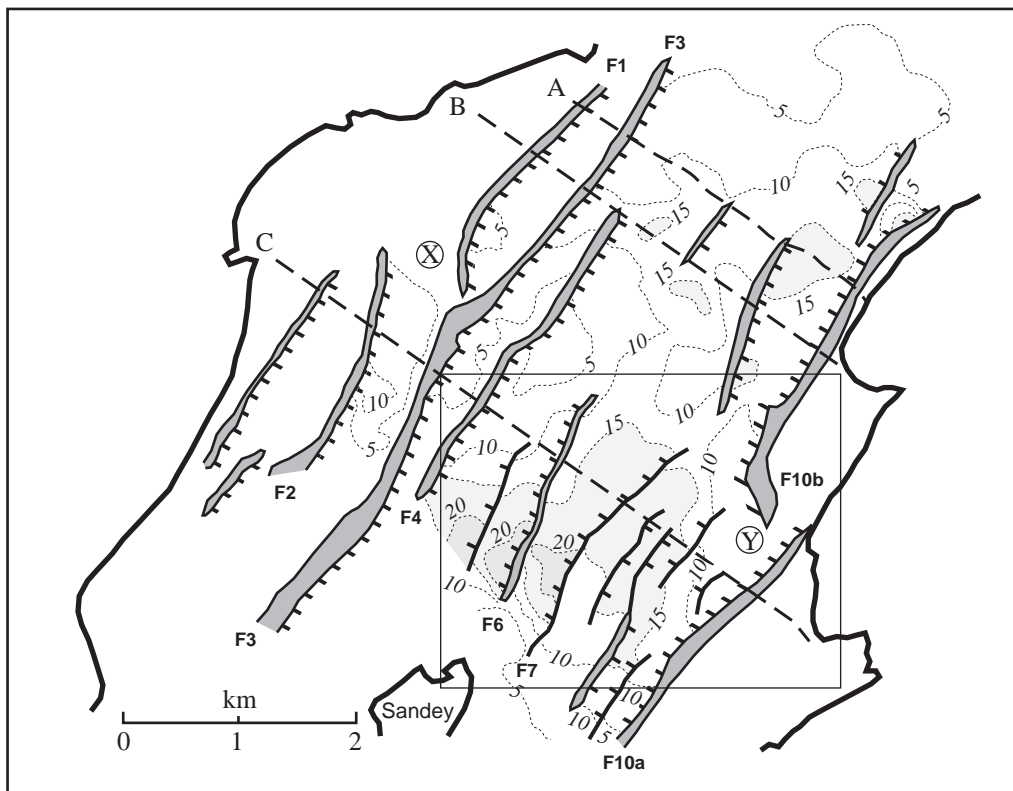
Fig. 1. Bathymetric map with contours in metres. The positions of major normal faults, identified from the Chirp profiler and sidescan sonar data, are indicated by elongate striped areas. Faults on the western side of the lake dip towards the east and those on the eastern side towards the west (sense indicated in Fig. 2). The width of the fault legend represents the superficial widths on sidescan sonar and chirp records, which we use as a proxy for fault heave. Dark shading around Sandey indicates approximate lakebed extent of the scoria cone. Light grey shading shows the extent of the 9.1 ka lava flow (Thingvallahraun). Intermediate shading in the southern part of the lake mark the 1.9 ka (Nesjahraun) lava. Positions of Chirp profiles are indicated by dotted lines. The positions of the prominent fissure swarms (Almannagja and Hrafnagja) at the northern end of the lake are indicated. Inset shows location of lake (T) on plate boundary zone in Iceland. Stipple indicates volcanic zones, and the arrows describe the relative plate motion (DeMets *et al.* 1994).

Fig. 2. Total sediment thickness (in ms two-way time) above the 9.1 ka lava. This thickness was derived from Chirp sub-bottom profiler data, together with major normal faults for the area indicated in Figure 1. Faults are shown where they offset the lava, and the tick marks are in the direction of down-throw. Dashed lines locate three profiles illustrated in Figure 3. Box outlines the area of Figure 4.

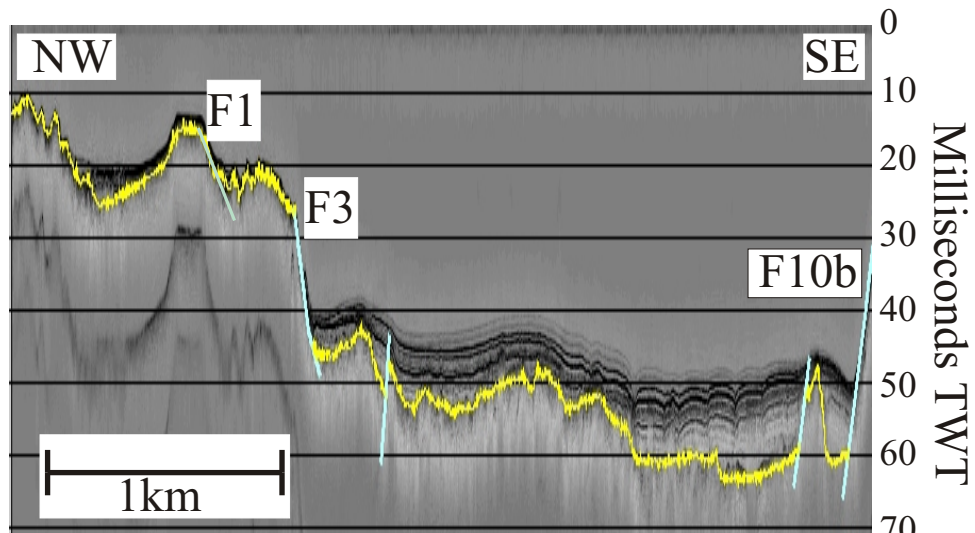
Fig. 3. Three representative Chirp sub-bottom profiles across the lake (see Fig. 2 for locations). These have a vertical exaggeration of c. 30:1. The 9.1 ka lava flow is indicated by the yellow horizon, while faults are marked in blue. The major western fault (F3) is marked, as is the major eastern boundary faults (F10a and F10b). Inset on profile C shows the horizons used to produce the isopach maps illustrated in Figure 4. Note within the inset that brown-yellow interval thins on both the foot-wall and hanging-wall of the faults, indicating that faulting could have developed by folding and uplift, as the fault tip propagated upwards.

Fig. 4. Isopach maps (in ms two-way-time) for time periods since 9.1 ka. These illustrate the changing loci of sedimentation since 9.1 ka within the part of the lake graben located in Figure 2. Upward propagation of faults is illustrated by the changes in detailed fault planforms between the periods recorded by the isopach maps (e.g. F5, F8 and F9). See main text for further discussion.

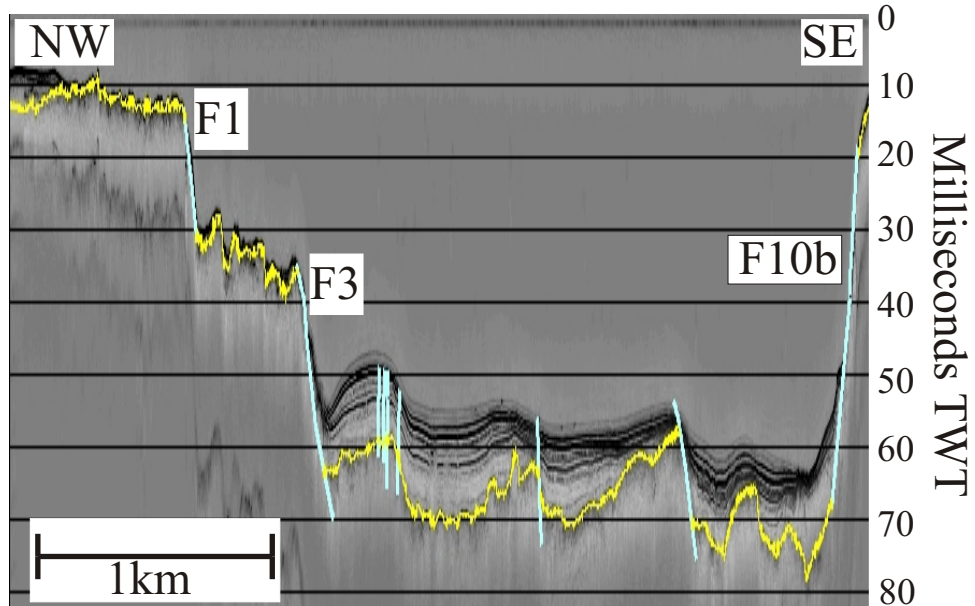




A



B



C

